Twenty-Fourth Symposium (International) on Combustion/The Combustion Institute, 1992/pp. 279–285

COMPARISON OF A MONTE CARLO PDF/FINITE-VOLUME MEAN FLOW MODEL WITH BLUFF-BODY RAMAN DATA

S. M. CORREA
General Electric Research Center
Schenectady, New York 12301 USA

AND

S. B. POPE
Cornell University
Ithaca, New York, 14853 USA

A hybrid Monte Carlo pdf/finite-volume mean flow model is developed and its predictions are compared with Raman data for a non-premixed, axisymmetric, bluff-body stabilized, 27.5% CO/ 32.3% H_2/ 40.2% N_2 - air flame. The velocity-composition joint pdf evolution equation is solved by an explicit Lagrangian Monte Carlo method. This joint pdf is iteratively adjusted in velocity sub-space to agree with the mean velocity fields given by the implicit finite-volume CFD procedure for the elliptic equations. Stochastic Lagrangian particle evolution occurs at a frequency obtained from the field solutions of turbulence kinetic energy and dissipation rate equations. The mean density field obtained from the pdf calculation is passed back to the finite-volume sub-model, and the hybrid algorithm is iterated to convergence. The composition is described by two scalars, which are the mixture fraction and a reaction progress variable for the partially equilibrated oxyhydrogen radical pool. Comparisons are made with Raman data on mean and rms mixture fraction fields, temperature, and major species, with good agreement. The hybrid method combines the accuracy of the pdf approach for turbulence-chemistry closure with the geometric flexibility of pressure-corrected finite-volume methods for mean flow in curvilinear coordinates. Standard limitations of pdf shape assumption and statistical independence of scalars, and of gradient diffusion, are removed.

Introduction

Two developments over the last several years have combined to challenge non-premixed turbulent combustion models, which have reached great sophistication in application to jet flames. First, the jet-in-coflow configuration is being replaced by recirculation-stabilized flames so as to provide stronger turbulence-chemistry interactions.[1–3] Unfortunately, the parabolic form of the transport equations is then replaced by the elliptic form. Practical flowfields are also often characterized by elliptic equations. Second, issues such as (a) blowoff and ignition, (b) NO_x, CO and unburned hydrocarbon pollutants, and (c) combustion efficiency, require multiple thermochemical variables for adequate description.[4] The standard pressure-corrected mean Navier-Stokes/assumed-shape pdf/k-ϵ turbulence model does not account rigorously for the turbulence-chemistry aspects of these issues, but affords significant geometric flexibility and rapid convergence for pressure-dominated internal flow.[5] On the other hand, while the Monte Carlo velocity-composition joint pdf transport model has been very successful in jet flames,[6,7] its numerical implementation is less well developed for recirculating flow or for flow within domains of complex shape; in the latter case the wall shape has a dominant effect on the mean pressure field. Here we combine the two methods using an approach similar to that of Refs. 8 and 9, and compare our results with Raman data from a non-premixed axisymmetric bluff-body stabilized 27.5% CO/ 32.3% H_2/ 40.2% N_2 - air flame.[3]

Formulation of Model

The starting point for the model is the Navier-Stokes equations and the partial-equilibrium thermochemical model, which assumes that the radical pool shuffle reactions are in partial equilibrium and that only the kinetics of the recombination reactions need to be accounted for. This thermochemical model has been used for CO/H_2 turbulent jet "diffusion" flames.[6,7] The mass fractions of major species and radicals, the density, and the temper-

ature, can be represented by the mixture fraction ξ and a combined variable $Y^*_{H_2}$. ξ is defined as usual in terms of elemental mass fractions Z_i and total enthalpy, normalized by the values in the fuel ("f") and air ("a") streams

$$\xi \equiv \frac{Z_i - Z_i^a}{Z_i^f - Z_i^a} \quad \text{for } \textit{each element } i\textit{, total enthalpy} \tag{1}$$

The combined variable $Y^*_{H_2}$ is given by

$$Y^*_{H_2} = Y_{H_2} + \frac{1}{2}\frac{M_{H_2}}{M_{OH}} Y_{OH} + \frac{M_{H_2}}{M_O} Y_O + \frac{3}{2}\frac{M_{H_2}}{M_H} Y_H + \frac{M_{H_2}}{M_{CO}} Y_{CO}. \tag{2}$$

where M_j and Y_j are the molecular weight and mass fraction, respectively, of species "j." The formation rate of this variable becomes independent of the shuffle reactions, depending only on the recombination reactions. Sometimes $Y^*_{H_2}$ is further normalized to yield a radical pool reaction progress variable, but here it is more useful in its original mass-specific form.

The turbulent flow is described by the velocity $\vec{U}$, the mixture fraction ξ and the variable $Y^*_{H_2}$. In the pdf transport equation, the velocity, mixture fraction and combined mass fraction variable become the independent variables denoted by $\vec{V}$, ψ, and Ω. A one-point statistical description in terms of the joint pdf of $\vec{U}$ and the scalars (ξ and $Y^*_{H_2}$) is sought. If the flow is statistically stationary, all one-point statistics depend only on the spatial coordinates.

The joint pdf $P(\vec{V}, \psi, \Omega)$ is the probability density of the simultaneous events $\vec{U} = \vec{V}$, $\xi = \psi$ and $Y^*_{H_2} = \Omega$ at that location in space and time. All one-point statistics are recovered from this pdf because the composition is a known function of ξ and $Y^*_{H_2}$. The velocity-composition joint pdf evolution model relaxes many of the assumptions made in the standard closure, such as pdf shape, statistical independence of scalars, and gradient diffusion of scalars. Closure of the non-linear chemical source term or "turbulent" fluxes of scalars are given directly by the pdf.

The modeling involved in the velocity-composition joint pdf equation is described by Pope.[10,11] Turbulent mixing of the scalars is modeled as a linear, deterministic relaxation to the local mean. The associated model constant (defined in Ref. 11) takes the standard value $C_\phi = 2$. For the velocity, the fluctuating component of acceleration (arising from the fluctuating pressure gradient and viscous forces) is modeled by the simplified Langevin model with the standard constant $C_o = 2.1$.[12] The joint pdf evolves in a five-dimensional velocity-composition space, u-v-w-ψ-Ω, beyond the two-dimensional physical space of the finite volume method, and so an explicit Lagrangian Monte Carlo solution technique is used.[10] The joint pdf is represented by a large number N of notional particles ($N \simeq 115{,}000$). At time t, the n^{th} particle has axial position $x^{(n)}(t)$, radial position $r^{(n)}(t)$, velocity $\vec{U}^{(n)}(t)$ and composition $\xi^{(n)}(t)$, $Y^{*(n)}_{H_2}(t)$. Inflow boundary conditions on the velocity, ξ, and $Y^*_{H_2}$ are specified at the jet and annular flow inlets, using values appropriate to each stream.

On each time step, the fields of the mean velocity and the turbulence frequency, obtained from the local turbulence kinetic energy and dissipation rate, are passed from the finite-volume sub-model to the pdf sub-model. A small correction (consisting of a shift and a uniform stretching in velocity space) is applied to the pdf so that the mean velocity and the turbulent kinetic energy of the two sub-models are in agreement. In this way, the no-slip boundary condition is automatically satisfied at all walls. Stochastic Lagrangian particle evolution occurs at the above frequency. The mean density field obtained from the pdf sub-model is passed back to the finite-volume sub-model, and the two "halves" of the hybrid algorithm are iterated to convergence. The convergence criterion is a statistical steady-state in the pdf method and reduction of residual errors by several orders of magnitude in the finite-volume method (the usual definition).[5]

Details of the implicit finite-volume calculation method for the mean flow are available in Ref. 5. Here continuity, mean axial and radial momentum, and turbulence kinetic energy and dissipation rate are solved for. The main features are:

1. Meshing: The domain is covered with a non-uniform cylindrical mesh which is numerically transformed to a uniform mesh. The transformed mean flow equations are solved on the latter mesh.
2. Staggered Grid: Variables are not defined at the same mesh points. Scalar variables such as pressure and density are located at common mesh points. Offset half a mesh-spacing to the left and below are the (axial) u and (lateral) v velocity points, respectively (in three dimensions, w is similarly staggered). This configuration stabilizes the pressure-velocity coupling.
3. Control Volume Formulation: The partial differential equations are integrated over control volumes centered on each grid point. On the staggered grid, the velocity and scalar values are located exactly where they are needed—at the

surfaces of the control volumes. This formulation ensures global conservation.

4. Discretization Schemes: Discretization of the convection terms can be one of the principal sources of error in numerical solutions of high Reynolds number flow.[5] The non-uniform 76 (axial) × 61 (radial) node grid used here is identical to that in Ref. 3, and the mean velocity and density fields are similar enough that the cell Reynolds and Peclet numbers are about the same (to well within 10%). As shown in Fig. 4 of Ref. 3, this mesh spacing is fine enough to reduce the transverse cell Reynolds/Peclet numbers to well below two in the important shear regions. Second-order central differencing could therefore be used without violating stability limits—if Pe > 2, explicit stabilization or first-order upwinding would be needed—and so freed the calculation from "numerical diffusion" error.[5]
5. Pressure-correction Algorithm: The continuity and momentum equations are manipulated to produce an equation for the mean pressure field, which is not available from the pdf equation. This equation is solved simultaneously with the other mean flow equations. The mean velocity field is "corrected" to conform to the mean pressure field, on every iteration. The algebraic equations that are the result of discretization are cast into a tridiagonal form and solved by line relaxation using the tridiagonal matrix algorithm.

The code was compiled in vectorized form and run on a CONVEX C240 mini-supercomputer. Execution proceeded at an estimated 5 MFlops, requiring approximately ten hours for this 75 × 60 cell, ~1.15 × 10^5 particle calculation. For display purposes, lower moments such as the means were averaged over the last 200 time-steps (out of 2000) of the pdf evolution, after a statistical steady-state was achieved. This significantly reduces the statistical fluctuations in the results.

Comparison with Raman Data

The bottom half of Fig. 1 shows the bluff-body burner in the wind-tunnel. The wind-tunnel is 15.2 cm × 15.2 cm in cross-section and was represented in this axisymmetric calculation by a circular cross-section of equal area. Since the tunnel dimension is much greater (×4) than the bluff-body diameter, this approximation is valid. The top half of Fig. 1 shows the computed mean velocity field in the vicinity of the jet exit. The off-axis stagnation zone and the region of high shear at $x/d \leq 10$ are evident ("d" ≡ jet exit diameter). Comparisons with the Raman data are made at $x/d = 10$ and 20.

Discussions of the Raman scattering apparatus and data reduction techniques, as well as comparisons of Raman data with a calculation of the bluff-body stabilized flame by the assumed shape *pdf*/k-ϵ method, are available in Ref. 3 and will not be repeated here. The same Raman data are used here.

Centerline profiles of the mean and r.m.s. of mixture fraction agree with the data except in the region beyond $x/d = 20$, where the predicted jet decay rates and turbulence levels are too low (Fig. 2). Radial profiles of the mean mixture fraction at $x/d = 10$ and $x/d = 20$ (Fig. 3) exhibit the correct peak value and width; the latter profile is less diffusive than the data suggest. These comparisons are affected by choice of the pdf model constant C_ϕ, which controls scalar dissipation. The r.m.s. of mixture fraction at $x/d = 10$ (Fig. 4), normalized by the mean, agrees with the data except in the outer edges where the mean is very small. The comparison on mean temperature is excellent (Fig. 5), well within what might be expected of the partial equilibrium model.

Figures 6–9 compare calculations and Raman data at $x/d = 10$ and 20, for the mean H_2, CO, H_2O, and CO_2, respectively. Mean H_2 and CO are predicted very well. The H_2O profiles exhibit discrepancies in the peak but not in the shapes of the profiles, with the location of the off-axis peak being resolved well. These discrepancies are attributable in part at least to the assumption of partial equilibrium in this relatively cool rich part of the flame. The comparison on CO_2 is worse; an additional contributing factor is the difficulty of making Raman measurements of this species.[3]

In general, the level of agreement is similar to or better than that obtained with the assumed shape pdf model.[3] Experimental data that would help further development of the theory include Laser Doppler Velocimetry (LDV), minor species measurements (e.g., by laser induced fluorescence, "LIF"), joint minor-major species measurements (e.g., LIF-Raman), and scalar fluxes (e.g., joint LDV-Raman). Post-processing for scalar fluxes, scalar-scalar correlations, and scatterplots will provide critical evaluation of the assumptions made in simpler methods.

Discussion

The computations are successful in providing a converged solution to the pdf transport equation, with the numerical errors being acceptably small. There is considerable scope, however, for increasing the efficiency of the method. Three salient considerations are:

1. To be accurate, the finite-volume method requires a fine grid, while the Monte Carlo method requires a large number of particles. Approximately 85% of the computational time was used

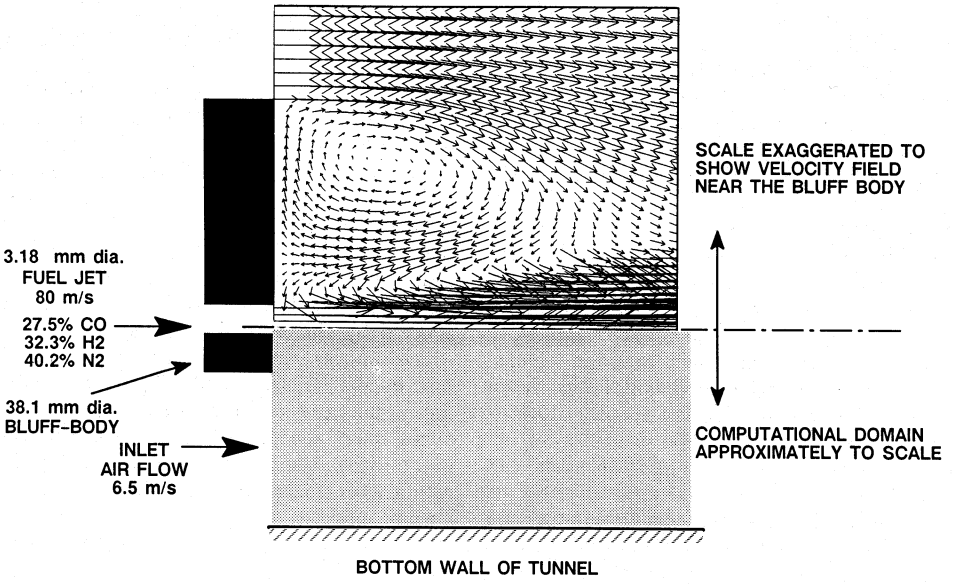

FIG. 1. Schematic of the bluff-body burner in the tunnel. Top half: Magnified view of velocity field near the bluff-body showing the region of high shear. Bottom half: inlet conditions and geometry.

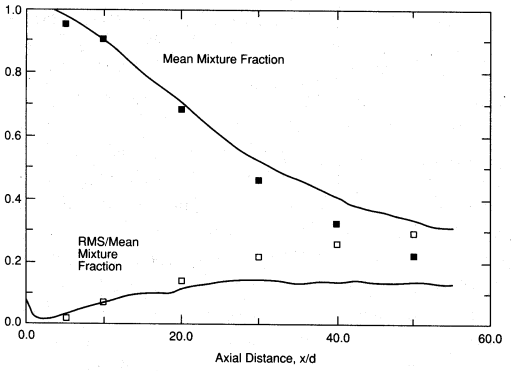

FIG. 2. Centerline profiles of mean and r.m.s. of mixture fraction compared with Raman data. "d" is the jet exit diameter. Symbols: experimental data;[3] lines: present calculations.

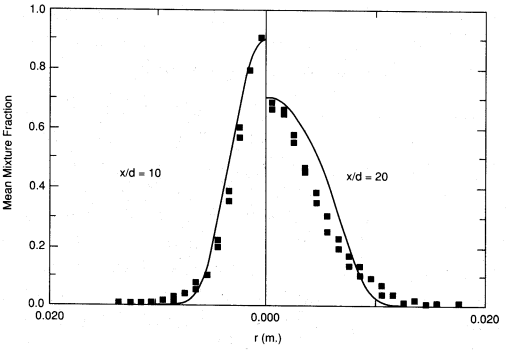

FIG. 3. Radial profiles of mean mixture fraction at x/d = 10 and 20. The calculated profiles extend to the tunnel wall (r = 0.085 m), but are truncated here to magnify the regions of interest. Raman data were obtained in vertical scans through the centerline, and data from both "sides" of r = 0 are included at each axial station. Symbols: experimental data;[3] lines: present calculations.

in the particle algorithm. Methods for balancing between each algorithm so as not to over-compute in either, beyond the error limits of the other, are required.

2. Parallel processing methods are well suited to both parts of the hybrid algorithm, and could significantly reduce the computational time.
3. The Monte Carlo method converges to a steady state in the statistical sense but, with a finite number N of particles, the estimated mean fields contain a statistical error of order $N^{-1/2}$. Various filtering techniques can be developed to reduce this error. Here time averages over 200 time steps of each quantity (mean and r.m.s. of mixture fraction, mean temperature, etc.) were presented. This has the effect of significantly increasing the effective number of particles.

While the agreement between the calculations and

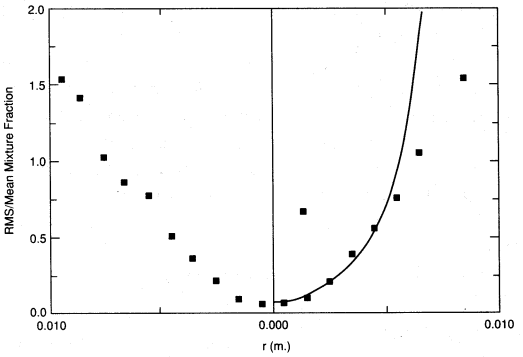

FIG. 4. Radial profile of r.m.s. of mixture fraction at $x/d = 10$. The full measured radial profile is shown.

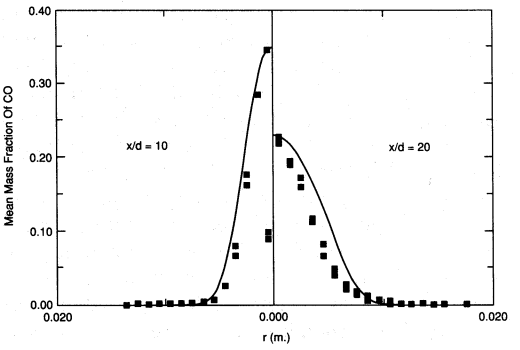

FIG. 7. Radial profiles of mean CO mass fraction at $x/d = 10$ and 20. Predictions and data plotted as in Fig. 3.

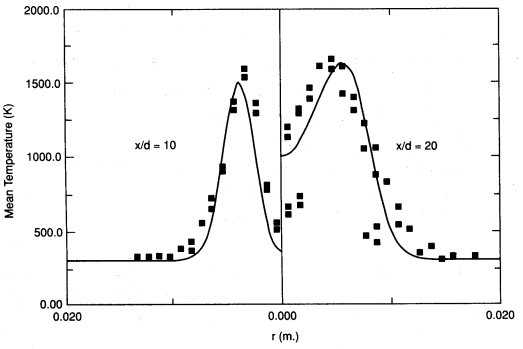

FIG. 5. Radial profiles of mean temperature at $x/d = 10$ and 20. Predictions and data plotted as in Fig. 3.

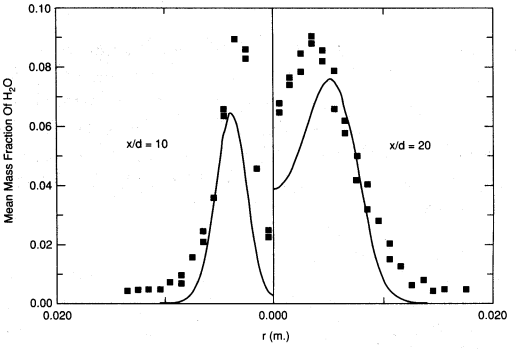

FIG. 8. Radial profiles of mean H_2O mass fraction at $x/d = 10$ and 20. Predictions and data plotted as in Fig. 3.

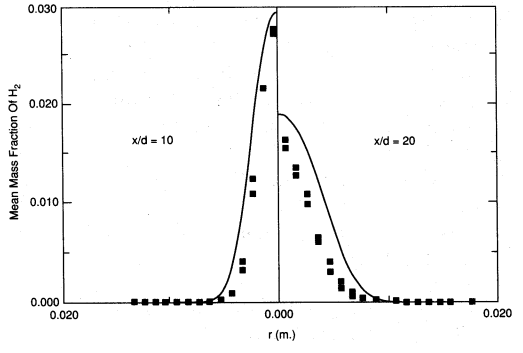

FIG. 6. Radial profiles of mean H_2 mass fraction at $x/d = 10$ and 20. Predictions and data plotted as in Fig. 3.

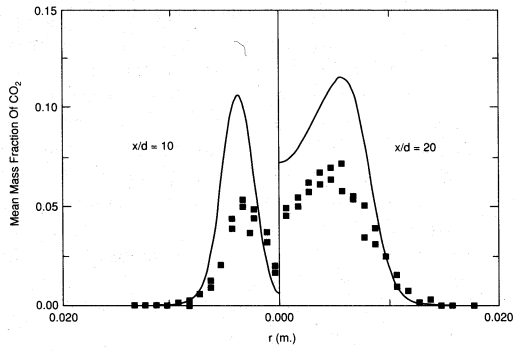

FIG. 9. Radial profiles of mean CO_2 mass fraction at $x/d = 10$ and 20. Predictions and data plotted as in Fig. 3.

measurements is very encouraging, it should be recognized that more accurate pdf models and more accurate thermochemical models are available; these, presumably, would improve the level of agreement. The simplified Langevin model used in the velocity pdf corresponds (at the Reynolds-stress level) to Rotta's model. Improvement is to be expected from the use of the generalized Langevin model which includes "rapid pressure" terms.[12] Without much cost—either in coding effort or in run time—the number of thermochemical variables can be increased from two to three or four, and thus more accurate thermochemical models can be used. Simplified kinetic schemes based on intrinsic low-dimensional manifolds are particularly well-suited for use with pdf methods.[13,14]

Conclusions

To obtain higher turbulent strain rates than attainable with jet flames, bluff-body stabilized burners are increasingly being used. Conventional assumed shape pdf methods and shear layer turbulence models such as k-ϵ will be insufficiently accurate to study these flows. The principal conclusions of this work are:

1. The hybrid algorithm, consisting of Monte Carlo solution of the joint pdf transport equation simultaneously with a finite-volume solution for the mean flow, combines the accuracy needed for turbulence-chemistry closure with the geometric flexibility of conventional CFD in curvilinear coordinates. (The latter capability was not demonstrated, being unnecessary in this simple geometry.) Gradient diffusion or second-order flux models for scalars are not required. By proper placement of grid, and refinement as necessary, numerical diffusion in the mean hydrodynamic field calculations can be eliminated or reduced to acceptable levels, at least in 2D.
2. With chemistry described by the two-scalar partial equilibrium model, the calculations were compared with Raman data previously obtained in a non-premixed bluff-body stabilized $CO/H_2/N_2$ flame. Agreement was very encouraging on mixture fraction mean and variance, temperature, and species concentration fields. Errors in the major species were attributable to a breakdown of the partial equilibrium assumption at temperatures below 1000 K.
3. The flexibility to handle multi-scalar kinetic schemes, without the realizability constraints imposed by assumed shape pdf's, can be exploited to model CO/H_2 flames more accurately,[13,14] or to model methane flames (e.g., with four scalars[15]).
4. Most of the computational time was taken by the explicit Monte Carlo particle-tracking algorithm. Future efforts will address the balancing of (i) the cell size required for accurate discretization of the mean field equations and (ii) the particle count required for accurate statistics.

Acknowledgements

The work at GE is supported in part by the Air Force Office of Scientific Research, Contract F49620-91-0072, Dr. Julian Tishkoff, Project Manager. The authors thank J. S. Sober for help with programming the CONVEX.

REFERENCES

1. Mansour, M. S., Bilger, R. W. and Dibble, R. W.: Twenty-Second Symposium (International) on Combustion; p. 711, The Combustion Institute, 1989.
2. Schefer, R. W., Namazian, M. and Kelly, J.: Twenty-Second Symposium (International) on Combustion, The Combustion Institute, p. 833, 1989.
3. Correa, S. M. and Gulati, A.: Measurements and Modeling of a Bluff-Body Stabilized Flame, Combust. Flame, 89, p. 195, (1992).
4. Correa, S. M.: A Review of NO_X Formation Under Gas-Turbine Combustion Conditions, Combust. Sci. Tech., in press, 1992.
5. Correa, S. M. and Shyy, W.: Prog. Energy and Comb. Sci., 13, p. 249 (1987).
6. Pope, S. B. and Correa, S. M.: Twenty-First Symposium (International) on Combustion, p. 1341, The Combustion Institute, (1987).
7. Correa, S. M., Gulati, A. and Pope, S. B.: Combust. Flame, 72, p. 159 (1988).
8. Anand, M. S., Pope, S. B. and Mongia, H. C.: in Turbulent Reactive Flows, Lecture Notes in Engineering, Vol. 40, Springer-Verlag, Berlin, p. 672, 1989.
9. Haworth, D. C. and El Tahry, S. H.: AIAA J., 29, p. 208, (1991).
10. Pope, S. B.: Prog. Energy and Comb. Sci., 11, p. 119, 1985.
11. Pope, S. B.: Twenty-Third Symposium (International) on Combustion, p. 591, The Combustion Institute, 1990.
12. Haworth, D. C. and Pope, S. B.: Physics of Fluids, 29, p. 387 (1986).
13. Maas, U. and Pope, S. B.: Simplifying Chemical Kinetics: Intrinsic Low-Dimensional Man-

ifolds in Composition Space, Combust. Flame, 88, p. 239, 1992.
14. MAAS, U. AND POPE, S. B.: Implementation of Simplified Chemical Kinetics Based on Intrinsic Low-Dimensional Manifolds, submitted to Twenty-Fourth Symposium (International) on Combustion, The Combustion Institute, in press.
15. CHEN, J.-Y., KOLLMAN, W. AND DIBBLE, R. W.: Combust. Sci. Tech., 64, p. 315 (1989).

COMMENTS

Cesar Dopazo, University of Zaragoza, Spain. It is well known that the LMSE scalar-mixing model has serious drawbacks such as the lack of relaxation of the PDF shape and the incorrect prediction of third and higher order moments. These limitations might be particularly critical in turbulent combustion where the accurate prediction of high order moments seems essential. Is your use of the LMSE model a first attempt in order to keep the computational cost as low as possible? Is your scalar-decay characteristic frequency identical for all Monte Carlo particles or different for each of them? How is it related to the turbulence frequency?

Author's Reply. It is certainly true that for the simple case of a decaying homogeneous scalar field the LMSE mixing model has the drawbacks you mention. As you yourself have pointed out in the past, for inhomogeneous flows there are other processes that may mitigate these shortcomings. While better mixing models are desirable, there is no evidence that other existing models (e.g., stochastic mixing models) perform better in this type of flow.

The scalar decay rate is $C_\phi\ \epsilon/k$, which depends on position, but is the same for all particles at a given location.

•

John Boersma, University of Twente, The Netherlands. My question concerns the chemistry model you use. In your previous work it contained also the reaction

$$CO + O + M \rightarrow CO_2 + M$$

Why don't you consider a separate reaction progress for CO and could this be a reason for the observed discrepancy between measured and calculated CO.

Author's Reply. To facilitate comparison with Ref. 3, the two-scalar chemistry model used here assumes that CO + OH = CO_2 + H is in equilibrium.

(i) The particular reaction you cite is not important for CO oxidation if H is present.

(ii) A reaction progress variable could indeed be used for CO + OH = CO_2 + H, adding one scalar to the system, but in fact

(iii) There is no significant discrepancy between measured and calculated CO. Clearly, the assumption of partially-equilibrated CO was reasonable.

•

Mehdi Namazian, Altex Technologies Corp., USA. Your model experiment comparisons were made at a low air to jet velocity ratio, where the flame is similar to a jet. Can the model predict high fluctuations which are observed when air to jet velocity is unity or greater than one?

Author's Reply. The jet-dominated regime was chosen in the experiments and therefore in our calculation, to avoid periodic shedding off the bluff-body; note that the off-axis mixing rates are higher than in a pure jet. The model would be expected to work in the unsteady regime you refer to, if an unsteady CDF and appropriate boundary conditions were substituted for the present steady ones.

•

A. R. Masri, The University of Sydney, Australia. The bluff-body flames with which you have compared your calculations:

(i) How far are they from global blow off?

(ii) Do they blow off at the jet exit plane or in the "neck" region downstream of the recirculation zone?

Author's Reply. Temperature-mixture fraction scatter plots of the CO/H_2 flame discussed here exhibit significant departures from adiabatic equilibrium, but little bimodality; these flames were far from global blowoff. Corresponding experiments with nitrogen-diluted methane exhibit significant bimodality in the "neck" region of the bluffbody flow.